SURFACE AND INTERFACE ANALYSIS
Surf. Interface Anal. 2005; **37**: 989–997
Published online in Wiley InterScience (www.interscience.wiley.com). DOI: 10.1002/sia.2095

SIA

Quantification of discrete oxide and sulfur layers on sulfur-passivated InAs by XPS

D. Y. Petrovykh,[1,2]* J. M. Sullivan[2,3] and L. J. Whitman[2]

[1] Physics Department, University of Maryland, College Park, MD 20742, USA
[2] Naval Research Laboratory, Washington, DC 20375-5342, USA
[3] Department of Chemistry, Northwestern University, Evanston, IL 60208, USA

Received 8 November 2004; Revised 7 April 2005; Accepted 7 April 2005

The initial quality and stability in air of InAs(001) surfaces passivated by a weakly-basic solution of thioacetamide (CH_3CSNH_2) is examined by XPS. The S-passivated InAs(001) surface can be modeled as a sulfur-indium-arsenic 'layer-cake' structure, such that characterization requires quantification of both arsenic oxide and sulfur layers that are at most a few monolayers thick. This thickness range complicates the quantitative analysis because neither standard submonolayer nor thick-film models are applicable. Therefore, we develop a discrete-layer model and validate it with angle-resolved XPS data and electron attenuation length (EAL) calculations. We then apply this model to empirically quantify the arsenic oxide and sulfur coverage on the basis of the corresponding XPS intensity ratios. Copyright © 2005 John Wiley & Sons, Ltd.

KEYWORDS: XPS; indium arsenide; InAs; thioacetamide; oxide; passivation; oxidation; coverage; attenuation

INTRODUCTION

Surface passivation of III–V semiconductors[1–5] has been a subject of intensive investigation for over a decade, primarily because of applications of these materials in microelectronics. More recently, chemical and biological sensing has emerged as another potential application for III–V semiconductors.[6,7] Inherent differences between sensing and electronic devices notwithstanding, both could benefit from the enhancements provided by surface chemical passivation. For example, a standard treatment using ammonium sulfide solutions $[(NH_4)_2S_x]$[2,3] produces S-passivated InAs surfaces with well-defined chemical and electronic properties, and short-term stability in air and aqueous solutions – a combination of properties which is required for sensing applications and which is also advantageous for microelectronics processing and fabrication.[7] One particularly promising alternative to inorganic sulfide passivation is treatment with solutions of thioacetamide (CH_3CSNH_2 or TAM hereafter).[8,9] For InAs(110), basic aqueous solutions of this organic sulfide have been reported to produce smaller roughness and more stable tunneling current (in scanning tunneling microscopy and spectroscopy) than the $(NH_4)_2S_x$ passivation.[10]

To examine the benefits of the TAM organic sulfide as a practical passivation approach for the technologically important InAs(001) surfaces, we use XPS to characterize the initial composition of TAM-passivated surfaces and their stability in air for up to 42 days. The remarkably efficient TAM passivation creates a surface with <1 monolayer (ML) of AsO_x – a coverage essentially undetectable in the As 3d region monitored in our previous work[7] (1 ML = 5.41×10^{14} atoms/cm^2 for bulk-terminated InAs(001)). We have found that the more surface-sensitive As 2p photoelectrons are required for characterization of such small amounts of AsO_x. In the passivation longevity study, the coverage of AsO_x and S extends from submonolayer to three MLs. Because the range cannot be covered by any single standard approximation used for XPS analysis, we have developed a discrete-layer (DL) model. Here we describe the details of the DL model, including its application to data from elemental core levels (As 2p, In 3d, S 2p), and the corresponding empirical AsO_x and S coverage calibrations. The application of the DL model for quantitative comparison between the TAM passivation and the $(NH_4)_2S_x$ benchmark is reported elsewhere.[11]

EXPERIMENTAL

Thioacetamide passivation of InAs(001) samples

InAs(001) samples (≈1 cm^2) were diced from a commercial single-side polished wafer (undoped, intrinsically *n*-type). We used commercial ACS reagent grade 99.0% thioacetamide (CH_3CSNH_2) and ACS PLUS grade 29.7% aqueous solution of NH_4OH. In-house triple-distilled water was used to dilute NH_4OH and rinse samples. We have explored a range of the TAM and NH_4OH concentrations and found that the optimal passivation was provided by the following solution: 0.2 g of TAM powder dissolved in 15 ml of the 1 : 9 volume

*Correspondence to: D. Y. Petrovykh, Code 6177, Naval Research Laboratory, Washington, DC 20375-5342, USA.
E-mail: dmitri.petrovykh@nrl.navy.mil
Contract/grant sponsor: Office of Naval Research.
Contract/grant sponsor: Air Force Office of Scientific Research.
Contract/grant sponsor: Defense Advanced Research Projects Agency.

mixture of the 29.7% NH_4OH stock solution and water. This standard TAM solution was used to prepare all the samples for the passivation longevity series. In contrast to passivation by $(NH_4)_2S_x$, we found that adding elemental sulfur[2,3,7] did not improve the efficiency of passivation by TAM.

Before passivation, InAs samples were degreased in acetone and ethanol (2 min in each solvent), rinsed in water, and blown dry under flowing nitrogen. The standard TAM solutions were heated to just below the boiling point (≈78 °C) in loosely capped glass vials placed in a waterbath. Upon heating, solutions became slightly yellow, and a pH between 11.0 and 11.5 was typically measured (using pH paper) after completing the passivation. Following a 4-min passivation in the standard TAM solution, each sample was rinsed for 2 min in copious amounts of water and blown dry under flowing nitrogen.

The shortest exposure to air was ≈5 min for a TAM-passivated sample that was transferred into an ultra-high vacuum (UHV) XPS chamber immediately after the final rinse in water. The longevity data were compiled from three separately prepared samples, each one measured two or three times at different time intervals up to 42 days and stored in a covered plastic wafer tray between the measurements.

XPS measurements

XPS measurements were performed in a commercial XPS system (Thermo VG Scientific Escalab 220i-XL) equipped with a monochromatic Al Kα source, a hemispherical electron energy analyzer (58° angle between the monochromator and analyzer), and a magnetic electron lens. (Certain vendors and commercial instruments are identified to adequately specify the experimental procedure. In no case does such identification imply endorsement by the Naval Research Laboratory.) Nominal X-ray spot size and analyzer field of view were $\leq$1 mm^2. The binding energies (BE) are reported with 0.1 eV precision, on the basis of a two-point analyzer energy calibration described in detail elsewhere.[12] Two types of normal-emission angle-integrated surveys were used to monitor samples for presence of contaminants: 0–1400 eV BE range (1.8 eV analyzer resolution, 1 eV point spacing), and 0–550 eV BE range (0.9 eV analyzer resolution, 0.33 eV point spacing). High-resolution normal-emission angle-integrated scans were acquired for the As 3d, In 3d, O 1s, C 1s, S 2p, and As 2p regions, with 0.36 eV analyzer resolution (0.9 eV for As 2p). In addition, high-resolution angle-resolved spectra were acquired at 35° and 65° (off-normal) emission angles for the As 3d, 2p, and In 3d regions. The nominal acceptance angles were 4° and 30° (along the energy dispersive and nondispersive directions respectively) for normal-emission angle-integrated measurements, and 5° for angle-resolved measurements. No specific effort was made to ensure a particular azimuthal alignment; all samples were positioned such that the tilt in angle-resolved measurements was approximately toward one of the easy cleavage directions, i.e. [110] or [1$\bar{1}$0]. XPS measurements were carried out at room temperature in a UHV chamber with base pressure of 1×10^{-9} Torr without any additional sample treatment.

XPS peak fitting

The peaks in the elemental core-level spectra were fit using commercial XPS analysis software.[13] A convolution of Lorentzian and Gaussian line shapes was used to fit the individual peaks. A linear combination of Shirley and

Table 1. Peak parameters from fits to high-resolution elemental XPS data for an InAs(001) surface S-passivated by the TAM treatment

Peak	Component	Emission angle (°)	BE[a] (eV)	Spin-orbit intensity ratio	Spin-orbit splitting (eV)	FWHM (eV)	
						Lorentzian	Gaussian
S 2p		0	161.6	0.52	1.17	0.12	1.00
In 3d	In-As	0	444.5	0.67	7.55	0.32	0.51
	In-S	0	445.0	0.67	7.55	0.32	0.51
	In-O_x	0	445.3	0.67	7.55	0.32	0.85
	In-As	35	444.6	0.69	7.56	0.31	0.49
	In-S	35	445.1	0.69	7.56	0.31	0.49
	In-O_x	35	445.4	0.69	7.56	0.31	0.76
	In-As	65	444.7	0.70	7.55	0.29	0.53
	In-S	65	445.2	0.70	7.55	0.29	0.53
	In-O_x	65	445.4	0.70	7.55	0.29	0.95
As 3d	As-In	0	40.7	0.68	0.71	0.13	0.57
	As-In	35	40.8	0.69	0.70	0.12	0.54
	As-In	65	40.9	0.68	0.70	0.23	0.46
As $2p_{3/2}$	As-In	0	1323.1			0.5	1.3
	As-O_x	0	1324.8			0.5	2.0
	As-In	35	1323.4			0.6	1.2
	As-O_x	35	1325.4			0.6	2.0
	As-In	65	1323.4			0.5	1.2
	As-O_x	65	1325.3			0.5	2.3

[a] For spin-orbit doublets, the BE is given for the higher intensity component.

polynomial functions was used to model the inelastic electron background, with the corresponding coefficients fit simultaneously with the peaks. Polynomial terms up to the second order were required to fit the nonlinear background in the In 3d, As 2p, and S 2p regions. The In-As, In-S, and In-O_x chemical components in the In 3d doublet were fit simultaneously for both In $3d_{5/2}$ and In $3d_{3/2}$ peaks. In these fits, the spin-orbit splitting and intensity ratio of the In $3d_{5/2}$ and In $3d_{3/2}$ peaks were left as free parameters, but the BE shifts and relative intensities of the chemical components were constrained to be identical between the In $3d_{5/2}$ and In $3d_{3/2}$ envelopes. Accordingly, only the fitting results for the In $3d_{5/2}$ peak are presented in the paper.

XPS RESULTS

We find that the TAM passivation treatment is remarkably efficient in removing the native oxide and preventing reoxidation – two key objectives of passivation.[7] Efficient native oxide removal is crucial because InAs samples are placed directly into the TAM solution without a preceding HCl-etch step typical for GaAs passivation.[1,4,5] The ability to prevent reoxidation and contamination in ambient determines the time available for carrying out any additional chemical steps.

The data in Plate 1 demonstrate the initial high-quality of TAM-passivated InAs(001). The survey spectrum (Plate 1(a)) is essentially identical to the one previously reported for $(NH_4)_2S_x$-passivated InAs(001) (compare to Fig. 1 in Ref. 7). The intensities of the surface contamination C 1s and O 1s peaks are comparable to those observed on a reference UHV-cleaved InAs(110) sample,[14] demonstrating how effectively the TAM-passivated surface resists both carbon and oxygen contamination in the ambient. The observed S 2p BE of 161.6 eV and full-width half-maximum (FWHM) of 1.1 eV (Plate 1(b), Table 1) are typical for a chemisorbed S layer on S-passivated InAs.[15,16] For the In 3d peaks in Plate 1(d), the surface In-S and In-O_x components appear as high BE shoulders, the intensity of which increases in the off-normal spectra. The fit shown for the In 3d 65° emission data (Plate 1(d), Table 1) is consistent with previously reported chemical shifts relative to the bulk In-As component: 0.45–0.50 eV for In-S and 0.7–1.0 eV for In-O_x.[7,15,16]

The salient feature of the angle-resolved As 3d spectra is the absence of As-O_x (BE = 44–45 eV) and As-S components (BE ≈ 43 eV),[7,15,16] even in the 65° emission spectra where surface sensitivity is enhanced. The absence of significant As-O_x confirms the high efficiency of the TAM passivation. The absence of an As-S component is also consistent with exclusive S binding to In, in agreement with a previously proposed 'layer-cake' structure model.[7] In the surface-sensitive As 2p region (Plate 1(c)), a small As-O_x component that is associated with surface oxide is observed, as indicated by the increasing As-O_x/As-In intensity ratio in off-normal data. The same As-O_x/As-In intensity ratio in the As 2p region can be used to track the long-term reoxidation following the TAM passivation, as shown in Plate 2(a) by representative spectra covering air exposure from 5 min to 42 days.

As shown by the In $3d_{5/2}$ fits in Plate 2(b), the In-S component slowly decreases with increased air exposure, while the In-O_x component increases. The increasing intensity of the high BE shoulder in the In $3d_{5/2}$ data makes deconvolution of the In-S and In-O_x components ambiguous, but consistent fits that agree both with the increasing oxidation trend seen in the As $2p_{3/2}$ data in Plate 2(a) and the slowly decreasing total S coverage seen in Plate 2(c) can be obtained. The S 2p data in Plate 2(c) suggest that the loss of S from passivated surfaces exposed to air proceeds through formation of volatile compounds, since S-O_x components do not appear in the S 2p region at any point in the passivation longevity series.

STRUCTURE MODEL AND PEAK ASSIGNMENTS

'Layer-cake' structure model

A simple 'layer-cake' structure model has been proposed to describe the S-passivated InAs(001) surface, whereby a stack of alternating In and As atomic layers is passivated by a layer of S chemisorbed on the In-terminated surface (Fig. 1(a)).[7] The model is consistent with chemical data from XPS, as well as structural information from coaxial-impact-collision ion-scattering spectroscopy and electron-diffraction observations.[3,7,15,17] This is an unusually simple structure for a S-passivated III-V semiconductor. In contrast, on the prototypical S-passivated GaAs(001) surface, both Ga-S and As-S components are observed, along with elemental As.[4,5,9] The nearly ideal In-S termination on InAs(001) is likely a result of solubility differences between In-S and As-S in the basic passivating solutions.[7]

Qualitatively, the chemical information from XPS data in Plate 1 support the extension of the 'layer-cake' model to TAM-passivated InAs(001). The BE and FWHM of the S 2p peak (Plate 1(b), Table 1) are consistent with a disordered chemisorbed S layer.[15,16] Deconvolution of the angle-resolved In 3d data indicates the presence of an In-S component (Plate 1(d), Table 1), while an As-S component is not observed (Plate 1(c) and 1(e), Table 1). The structure model and consideration of potential oxidation pathways (Fig. 1) suggest that developing a method for quantification

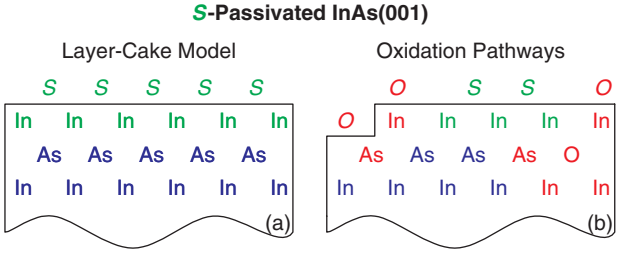

Figure 1. Schematic of a S-passivated InAs(001) surface. (a) The idealized 'layer-cake' structure model: alternating In and As atomic layers with the top In layer terminated by the passivating S layer. Note that the idealized structure involves exclusively In-S and not As-S bonding. (b) Potential oxidation pathways: displacement of S by O, oxidation of defects in the top In layer, oxygen diffusion through the protective layer.

of the AsO_x and S coverages is important for quantitative analysis of the surface structure as a function of treatment and time. First, we consider the appropriate choices of reference peaks for such quantification in the following text. In the 'Quantitative XPS Analysis' section, we introduce a DL model and then use it to interpret the experimental core-level peak ratios and to produce empirical AsO_x and S coverage calibrations.

Peak assignments and properties: As 3d, S 2p, and In 3d

The As 3d peak offers three features desirable for use in characterization of S-passivated InAs: high intensity, narrow FWHM, and large chemical shifts between the As-In, As-S and As-O_x components (Plate 1(e), Table 1). These were the reasons for previously choosing the As 3d region for characterization of reoxidation and band bending in our $(NH_4)_2S_x$-passivated InAs(001) study.[7] The superior efficiency of the TAM passivation in preventing reoxidation, however, results in As-O_x components close to the quantification limit in the As 3d region – even after a few days in air – and thus makes the As 3d region unsuitable for quantitative analysis of reoxidation. The stability of the As 3d signal actually makes it useful as an internal reference. As 3d photoelectrons have the highest kinetic energy (KE) among elemental core-levels in our dataset, and the corresponding electron attenuation length (EAL) is about five times larger than the 0.606 nm InAs lattice constant (see Appendix, Table A1), making the bulk As component the least affected by any changes in the top few surface layers. Accordingly, all elemental spectra in Plates 1 and 2 are normalized to the intensity of the corresponding bulk As 3d peaks.

The S 2p peak provides the most information about the S layer because different chemical states of S (i.e. physisorbed, chemisorbed, or oxidized) result in dramatically different S 2p BEs. A single S 2p peak (Plates 1(b), 2(c)) indicates a narrow distribution of chemisorbed S states on S-passivated InAs(001). Note that for chemisorbed S on InAs, the S 2p spin-orbit splitting is typically[15,16] not as pronounced as in spectra of highly ordered S layers (e.g. alkanethiol self-assembled monolayers on Au), indicating some disorder at the In-S interface. Because the KE difference between the S 2p and As 3d peaks is <10%, the S 2p/As 3d intensity ratio is expected to be rather insensitive to any surface changes above the S layer, such as oxidation and contamination in air, and, thus, can be used for the quantitative analysis of the time evolution of the total S coverage. For S 2p peak fitting, it is important to note that, for InAs samples, the background in the S 2p region is distinctly nonlinear and, thus, requires inclusion of appropriate nonlinear terms in the background fitting function (see the native oxide control spectrum in Plate 2(c)).

The In 3d peak is the most intense peak in spectra from InAs samples (Plate 1(a)). For S-passivated surfaces, it also contains the most chemical information, with both In-S and In-O_x components appearing along with the bulk In-As signal (Plate 1(d)). The small difference in chemical shifts between the In-S and In-O_x components (Plates 1(d), 2(b), Table 1) makes peak fitting ambiguous without additional constraints, as further discussed in the *S coverage analysis* section.

Surface-sensitive As 2p peaks: oxidation versus sulfidization signatures

The As 2p peaks (As $2p_{3/2}$ shown in Plates 1(c) and 2(a)) are the most surface-sensitive in the As spectrum due to the low KE of As 2p photoelectrons. In fact, the corresponding EAL is comparable to the InAs lattice constant (see Appendix), so the detected As 2p photoelectrons originate almost exclusively from the top few atomic layers and are very sensitive to surface composition. For example, the oxide component in Plate 1 can be clearly observed in the As 2p region but not in the As 3d region, in agreement with a previous report for residual oxide layers on GaAs.[18] As 2p photoelectrons are also sensitive to surface contamination, e.g. note the lower As 2p intensity from the passivated sample after 42 days in air *versus* the native oxide control in Plate 2(a) (two bottom spectra), the former sample had accumulated about three times more adventitious carbon, and thus the As 2p signal is stronger attenuated.

The interpretation of the high BE As 2p components warrants a special discussion. The native oxide control in Plate 2(a) shows a component shifted by ~4 eV. A comparison with the corresponding As 3d data (not shown) and literature values suggests that this component is a mixture of As^{3+} and As^{5+} oxides.[18,19] The passivated samples exposed to air for more than one day show the same ~4 eV chemical shift, indicating similar oxidation states (Plate 2(a)). However, the freshly passivated sample shows a high BE As 2p component with only a 2 eV shift (Plates 1(c), 2(a) and Table 1), smaller than the reported 3 eV shift for As^{3+} oxide.[19] The angle dependence shown in Plate 1(c) clearly indicates this is a surface As 2p component, and we attribute it to a sub-oxide associated with the initial limited oxidation. A BE shift with oxide coverage reported in a previous study of residual oxides on GaAs supports the sub-oxide interpretation of this As 2p component.[18]

For S-passivated InAs(001), we have to consider the possibility of an alternative assignment for the As 2p component shifted by 2 eV, as a 1.65 eV shift has been reported for As-S on GaAs(100) sulfidized in an aqueous $(NH_4)_2S$ solution (Fig. 1(a) in Ref. 20). Some As–S bonds can be expected on S-passivated InAs(001) because of imperfections in a layer-cake surface structure (Fig. 1). Since our energy resolution is insufficient to reliably separate such a putative As-S component from the As-O_x sub-oxide component discussed above, we can only place a reasonable upper limit on the two coverages by assuming that approximately half of the intensity corresponds to each As-S and As-O_x, a limit consistent with the S coverage quantification.

QUANTITATIVE XPS ANALYSIS

Standard overlayer/bulk intensity ratio models

The full expression for the normal-emission overlayer/bulk intensity ratio, I_{ov}/I_b, in the standard XPS formalism (adapted to include updated practical definitions of EALs[21,22]) is:

$$\frac{I_{ov}}{I_b} = \frac{T_{ov}}{T_b}\frac{\sigma_{ov}}{\sigma_b}\frac{L^Q_{ov}}{L^Q_b}\frac{N_{ov}}{N_b}\frac{\left[1-\exp\left(-\frac{t}{L_{ov}}\right)\right]}{\exp\left(-\frac{t}{L^b_{ov}}\right)} \qquad (1)$$

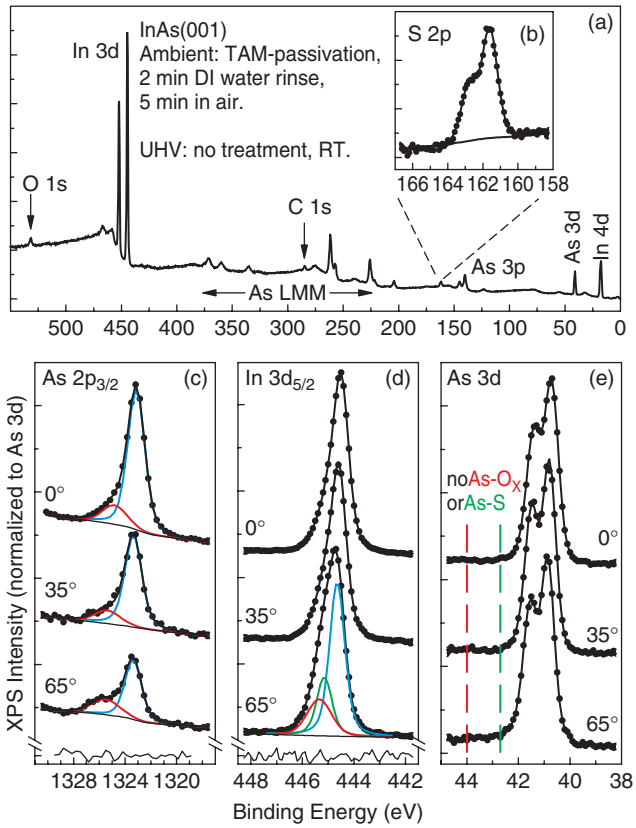

Plate 1. XPS data for an InAs(001) surface immediately after the TAM treatment. (a)–(b) The survey spectrum for InAs(001) immediately after TAM passivation and a high-resolution close-up of the S 2p region. (c)–(e) High-resolution angle-resolved elemental core-level data (emission angles as indicated). Deconvolution of the angle-resolved spectra shows surface components: As-O_x (red) in (c), and In-S (green), In-O_x (red) in (d). Symbols = raw data, thin lines = fit components and backgrounds, thick lines = fit sum curves, thin lines at bottom of (c) and (d) = fit residuals.

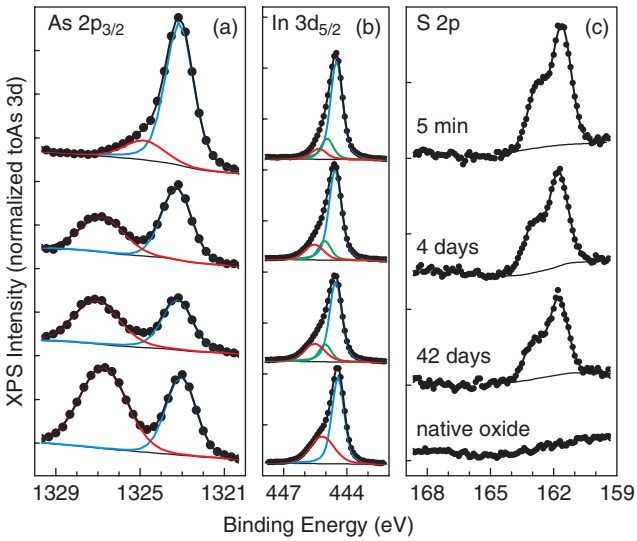

Plate 2. High-resolution elemental XPS data for TAM-passivated InAs(001) after exposure to air (normal-emission, angle-integrated, time in air as indicated). Bottom spectra in each panel are from a rigorously degreased InAs(001) wafer (native oxide control). (a) The As-O_x component (red) increases relative to As-In (blue) with increasing exposure to air. (b) The fit results are from the fixed In-S BE shift method (see text), and they show an In-O_x component (red) increasing and an In-S component (green) decreasing with time. (c) The intensity of the S 2p peak decreases with time in air; the FWHM remains constant. Note the absence of S-O_x features above 164 eV. Symbols = raw data, thin lines = fit components and backgrounds, thick lines = fit sum curves.

where T is the analyzer transmission function, σ is the total photoelectric cross-section,[23] N is the elemental atomic density, t is the overlayer thickness, L^{Q} is the ''EAL for quantitative analysis'' (QEAL) and L_{ov} is the ''average practical EAL'' (PEAL). A detailed discussion of the QEAL and PEAL definitions and calculations is presented in the Appendix. Equation (1) assumes that the two signals are acquired in parallel; thus, all the geometric factors and the X-ray flux cancel out in the intensity ratio. For an oxide overlayer, the two signals in Eqn (1) correspond to the two components of the same core-level peak separated by a small chemical shift; therefore $\sigma_{ox}/\sigma_b = 1$, $T_{ox}/T_b \approx 1$, $L^{b}_{ov} \approx L_{ov} = L_{ox}$ and Eqn (1) can be simplified:

$$\frac{I_{ox}}{I_b} = \frac{L^{Q}_{ox}}{L^{Q}_{b}} \frac{N_{ox}}{N_b} \frac{\left[1 - \exp\left(-\frac{t}{L_{ox}}\right)\right]}{\exp\left(-\frac{t}{L_{ox}}\right)} \tag{2}$$

A typical limiting case for Eqn (2) is a thick-film oxide approximation (ThF), where the prefactor is cancelled by assuming that the respective oxide and bulk properties are the same:

$$\frac{I_{ox}}{I_b} = \frac{\left[1 - \exp\left(-\frac{t}{L_{ox}}\right)\right]}{\exp\left(-\frac{t}{L_{ox}}\right)} \tag{3}$$

Equation (3) relates the experimental intensity ratio X and signal attenuation in the oxide R:

$$X = \frac{1-R}{R}, \text{ where } X = \frac{I_{ox}}{I_b} \text{ and } R = \exp\left(-\frac{t}{L_{ox}}\right) \tag{4}$$

Another limiting case for Eqn (2) is a submonolayer oxide approximation (SubML), where the signal attenuation in the oxide layer is assumed negligible ($R = 1$); $L^{Q}_{b}N_b$ represents the total number of substrate atoms contributing to the signal, and $L^{Q}_{ox}N_{ox}$ is replaced by the total number n_{ox} of oxidized atoms in the submonolayer:

$$\frac{I_{ox}}{I_b} = \frac{n_{ox}}{L^{Q}_{b}N_b} \tag{5}$$

Discrete-layer model

Both chemical intuition and our prior results suggest that the AsO_x and S coverages are between 1 and 3 ML on many samples in the longevity series of TAM-passivated InAs(001). For this coverage regime, however, neither of the two limiting approximations described above (Eqns (3–5)) is strictly applicable. Therefore, we develop a modified approach – the discrete-layer (DL) model shown schematically in Fig. 2. The general approach is to explicitly incorporate the generation of the oxide signal by a number of discrete (full or partial) atomic layers by replacing the numerator in Eqn (2) by a finite sum, while keeping the 'thick-film' approximation to describe the exponential attenuation of the substrate signal.

It is helpful to define several model parameters indicated in Fig. 2. The oxide overlayer is described by a number of full atomic layers α and a fractional coverage θ for the outermost layer. If a is the thickness of one full atomic layer, then

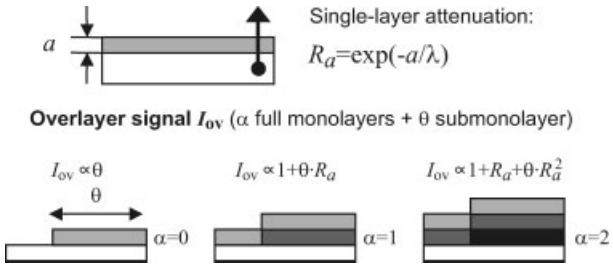

Figure 2. A discrete-layer model used for quantification of AsO_x and S overlayers. Photoelectrons passing through a single atomic layer of thickness a are exponentially attenuated with EAL λ by a factor R_a. For more than one full monolayer, contributions from lower layers are attenuated by each overlayer or a fraction θ thereof.

the total overlayer thickness t_{DL} for use in the 'thick-film' denominator can be approximated as:

$$t_{DL} = a(\alpha + \theta) \tag{6}$$

The corresponding single-layer (R_a) and total (R) attenuation factors are defined as:

$$R_a = \exp\left(-\frac{a}{L_{ox}}\right) \text{ and } R = (R_a)^{\alpha+\theta} \tag{7}$$

The substrate signal intensity is given by the 'thick-film' denominator of Eqn (2):

$$I_b \propto L^{Q}_{b}N_bR = L^{Q}_{b}N_b(R_a)^{\alpha+\theta} \tag{8}$$

The oxide signal is generated in a given discrete atomic layer, and it is attenuated by a factor of R_a for each oxide layer above it. This model gives the discrete oxide signal intensity dependence on the number of full oxide layers α (Fig. 2):

$$I_{ox}(\alpha = 0) \propto \theta, I_{ox}(\alpha = 1) \propto 1 + \theta \cdot R_a \text{ and}$$
$$I_{ox}(\alpha = 2) \propto 1 + R_a + \theta \cdot (R_a)^2 \tag{9}$$

For up to three ML coverage, the oxide/bulk intensity ratio can then be written in closed form as:

$$X = \frac{I_{ox}}{I_b} = \frac{n_{ML}}{L^{Q}_{b}N_b} \frac{\alpha + \theta \cdot (R_a)^{\frac{\alpha}{\cos\phi}} + \frac{\alpha(\alpha-1)}{2} \cdot \left[(R_a)^{\frac{1}{\cos\phi}} - 1\right]}{(R_a)^{\frac{\alpha+\theta}{\cos\phi}}}$$
$$\theta_{DL} = \theta + \alpha \tag{10}$$

where θ_{DL} is the total oxide coverage, the $1/\cos\phi$ exponent applied to the R_a attenuation terms accounts for the emission angle ϕ, $n_{ML} = 5.41 \times 10^{14}$atoms/cm^2 $\equiv$ 1 ML is the surface density of bulk-terminated InAs(001), and the expression in the numerator gives the appropriate results listed in Eqn (9) for $\alpha = 0, 1, 2$. The closed-form expression in Eqn (10) can be numerically solved for θ, given an experimental intensity ratio X, angle ϕ and the appropriate choice of the discrete parameter α. The L_{ox} (PEAL) and L^{Q}_{b} (QEAL) values have been calculated using the NIST SRD-82 software[21,22] as described in the Appendix and as listed in Table A1. For

quantification of the bulk In and As signals, the bulk atomic density $N_b = 1.80 \times 10^{22}$ atoms/cm^3 was assumed (i.e. one-half of the InAs bulk density). The ML thickness for the oxide was fixed at $a = 0.3$ nm, which is approximately one-half of the InAs lattice constant, and is the value that minimizes the difference between the solutions of Eqn (10) for 0° and 65° emission data from oxides of thickness >1 ML.

For As 2p photoelectrons, the 'bulk' intensity originates only in the top few substrate layers. Therefore, we examined if a ThF denominator in Eqn (10) provides a sufficiently accurate approximation. A full-discrete-layer (FDL) model accounts for both the discrete nature of the As layers that generate the signal in the 'layer-cake' substrate and the DL attenuation of the substrate signal. For a semi-infinite 'layer-cake' substrate, the sum of intensities from individual layers (effective attenuation length λ_{eff}, layer spacing $a_\perp = a_{InAs}/2 = 0.303$ nm) can be represented as a signal from an effective number of layers N_{eff}:

$$N_{eff} = \frac{1}{1 - \exp\left(-\frac{a_\perp}{\lambda_{eff}}\right)}, N_{eff} n_{ML} = L_b^Q N_b \qquad (11)$$

To obtain the FDL expression, the DL attenuation of the substrate signal by the oxide must be combined with Eqn (11); thus, the FDL denominator for Eqn (10) becomes:

$$I_b = N_{eff} n_{ML} \left[\exp\left(-\frac{a\alpha}{L_{ox}\cos\phi}\right)\right] \times \left\{1 + \theta\left[\exp\left(-\frac{a}{L_{ox}\cos\phi}\right) - 1\right]\right\} \qquad (12)$$

AsO_x coverage analysis

Table 2 presents the experimental I_{ox}/I_b intensity ratios measured for the As $2p_{3/2}$ peak in normal and 65° emission, and the corresponding coverages and thicknesses of the AsO_x overlayer calculated using the SubML model (Eqn (5)), the DL model (Eqn (10)), the FDL model (Eqns (10–12)), and the ThF model (Eqns (3–4)). The SubML and ThF models quantify the overlayer only in terms of the oxide coverage and thickness, respectively; the DL model results are shown using both metrics (related via Eqn (6)) for ease of cross-model comparison. The DL model coverages (Eqn (10)) were calculated from normal and off-normal emission intensity ratios; as the two values differed by <10%, their averages are listed in Table 2. Only the DL model results are presented in Table 2 for the As $2p_{1/2}$ data; the cross-model trends were essentially the same as those shown for As $2p_{3/2}$.

The data in Table 2 highlight several important features of the models. Most significantly, the DL and FDL models provide the best approximation for quantifying the oxide in this range of coverage/thickness, and show quantitative agreement with the SubML and ThF results for coverages <0.5 and >1 ML respectively. The SubML model by construction results in an estimate of the oxide coverage that is linear with the corresponding intensity ratios, and the combination of the cosine factor and the appropriate QEAL produce a reasonable agreement between normal and off-normal emission SubML results. The linear nature of the SubML model, however, causes it to severely overestimate coverages ≥0.5 ML. Conversely, the ThF model underestimates the oxide coverage for values <1 ML, as can be expected from a model that assumes a complete overlayer. The FDL coverages are systematically ~10% higher than the DL values, indicating that in this oxide thickness range the ThF denominator in Eqn (10) slightly underestimates the substrate signal attenuation compared to the FDL expression (Eqn (12)).

For practical applications of the DL and FDL models, we have calculated empirical As-O_x coverage calibration curves (Fig. 3) on the basis of the model parameters used for the As $2p_{3/2}$ data in Table 2. The DL model validation above (see also Table 2 above and the Appendix) suggests an uncertainty estimate of about 20% for these calculated coverage values.

Table 2. Oxide overlayer quantification for the TAM passivation longevity series

Time in air (days)	As $2p_{3/2}$ 0° I_{ox}/I_b	As $2p_{3/2}$ 0° θ^0_{SbML} (ML)[a,b]	As $2p_{3/2}$ 65° I_{ox}/I_b	As $2p_{3/2}$ 65° θ^{65}_{SbML} (ML)[a,b]	θ_{DL} (ML)[a,c]	θ_{FDL} (ML)[a,d]	t_{DL} (nm)[e]	t_{ThF} (nm)[f]	As $2p_{1/2}$ θ_{DL} (ML)[a,c]
0.004	0.184	0.42	0.413	0.39	0.40	0.44	0.120	0.076	0.39
0.017	0.198	0.45	0.619	0.58	0.47	0.52	0.141	0.081	0.47
0.729	0.462	1.06	1.060	0.99	0.72	0.77	0.217	0.170	0.80
3	0.459	1.06	1.243	1.16	0.75	0.79	0.225	0.169	0.84
4	0.694	1.60	1.526	1.43	0.90	0.92	0.269	0.235	1.01
33	1.137	2.61	2.219	2.07	1.18	1.20	0.353	0.339	1.18
42	1.263	2.90	2.494	2.33	1.26	1.31	0.378	0.365	1.37

[a] Surface density of bulk-terminated InAs(001) is used to define 1 ML = 5.41×10^{14} atoms/cm^2.
[b] Coverage calculated using the submonolayer model, Eqn (5).
[c] Coverage calculated using the discrete-layer model, Eqn (10).
[d] Coverage calculated using the full-discrete-layer model, Eqns (10–12).
[e] Thickness calculated from the discrete-layer model coverage θ_{DL}, Eqn (6).
[f] Thickness calculated using the thick-film model, Eqns (3–4).

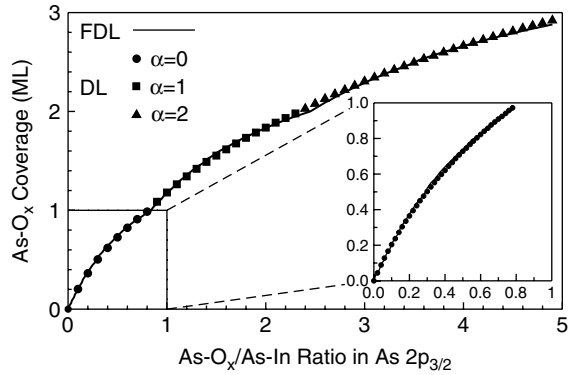

Figure 3. As-O_x coverage calibration calculated using the discrete-layer (DL) and full-discrete-layer (FDL) models for As-O_x/As-In component intensity ratio in the As $2p_{3/2}$ region (normal emission). Symbols indicate the number of complete oxide layers (α parameter in Eqn (10)); inset shows a close-up of the submonolayer coverage region.

S coverage analysis

The S coverage for the S-passivation longevity series can be estimated using two independent methods. The first method is to use the S 2p/As 3d intensity ratio (Table 3). Because of the S 2p and As 3d peak properties discussed in the previous section, this ratio is the best model-independent, semiquantitative measure of the S coverage,[11] even for samples with unknown distribution of elements in the top few atomic layers. The second method is to use In 3d and S 2p peaks for a quantitative coverage estimate. However, this approach relies on deconvolution of In 3d chemical components and assumptions about the surface structure and, thus, has more limited applicability than the first method.

A freshly passivated surface is the sample for which estimating the absolute S coverage is most important (Plate 1, top spectra in Plate 2). In order to use the DL model, we need a reliable method of fitting the In 3d chemical components: In-As, In-S, and In-O_x (Plates 1(d), 2(b)). We have tested two sets of fitting constraints: fixed BE shift for the In-S component only (Plates 1(d), 2(b)) and fixed BE shifts for both the In-S and In-O_x components. Using Eqn (10) and EAL values from Table A1, we calculated In-S and In-O_x coverages from components fit by the two methods: 1.5 ML of In-S, 1.2 ML of In-O_x (fixed In-S, Plate 1(d), Table 1), and 1.9 ML of In-S, 0.5 ML of In-O_x (fixed In-S and In-O_x). Comparing the In $3d_{5/2}$ data for increasingly oxidized samples in Plate 2(b), it appears that the In-O_x BE shift on the freshly passivated sample, which contains primarily sub-oxides, is smaller than that observed on the native oxide control. Fixing the In-O_x BE shift in a fit then would result in underestimating the In-O_x contribution for samples with very low oxidation. Conversely, the S coverage changes only by about one-third in the series; thus, the In-S BE shift should change very little and fixing it improves the consistency of the fits without introducing artifacts (Plates 1(d), 2(b), Table 1).

Table 3. Sulfur coverage analysis for the TAM passivation longevity series

Time in air (days)	S 2p/As_{As-In} 3d[a]	S 2p/In $3d_{5/2}$[b]	θ_S (ML)[c]
0.004	0.27	0.024	1.7
0.017	0.24	0.025	1.8
3	0.20	0.018	1.3
4	0.23	0.020	1.4
33	0.18	0.016	1.1
42	0.17	0.016	1.1

[a] Experimental intensity ratio: total S 2p to As-In component of As 3d.

[b] Experimental intensity ratio: total S 2p to In $3d_{5/2}$.

[c] S coverage calculated from S 2p/In $3d_{5/2}$ intensity ratios using Eqn (13), 1 ML = 5.41×10^{14} atoms/cm^2.

Clearly, a different quantitative method, that does not require deconvolution of the In 3d components, is desirable for tracking the S coverage over the entire longevity series. One approach is to modify Eqn (5) to include the element-specific photoelectric cross-section and transmission function ratios, σ_S/σ_{In} and T_S/T_{In}. The S coverage θ_S is then given by:

$$\theta_S = \frac{T_{In}}{T_S}\frac{\sigma_{In}}{\sigma_S}\frac{L^Q_{In}N_b}{n_{ML}}\frac{I_S}{I_{In}} \qquad (13)$$

where to produce the S coverage in ML, the numerical prefactor in front of the ratio of *total* S 2p and In $3d_{5/2}$ intensities I_S/I_{In} is 70.5.

For the freshly passivated sample, Eqn (13) gives θ_S = 1.7 ML (Table 3), in good agreement with the DL result (1.5 ML of In-S) and the upper limit of 0.2 ML of As-S obtained from the As 2p data. Note that the S coverage changes by ≈35% in the longevity series (Table 3). Given that Eqn (13) is quantitatively accurate for the first sample in the series, the linear nature of Eqn (13) suggests it should be approximately valid for the rest of the series. Equation (13) provides a better quantitative coverage estimate from the S 2p/In 3d intensity ratio than Eqn (5) did in the As-O_x/As-In 2p case because the total In 3d signal is contributed by both the bulk-dominated In-As component (QEAL = 2.43 nm) and the topmost In-S/In-O_x layers. However, it also means that the accuracy of this empirical quantification relies on the particular surface structure and thus may not be generally applicable.

CONCLUSIONS

We have used high-resolution angle-resolved XPS measurements to quantitatively characterize the initial structure and stability in air of InAs(001) surfaces passivated by thioacetamide. We find that the TAM treatment very effectively removes native oxide and passivates InAs(001) with a chemisorbed S layer against reoxidation and contamination in aqueous solutions and laboratory air. XPS elemental analysis and reoxidation behavior for TAM-passivated samples are consistent with the S/In/As 'layer-cake' structure model proposed for other S-passivated InAs(001) surfaces. The high efficiency of the TAM passivation resulted in very small amounts of As-O_x during the initial reoxidation and, thus, required the use of oxide/bulk intensity ratios from

the surface-sensitive As 2p region, and the development of a DL model for quantitative analysis of the measured intensity ratios. In addition, a method was developed for quantifying the S coverage on S-passivated InAs(001) on the basis of the analysis of S 2p and In 3d peak intensities. Quantitatively, the following components were identified on an InAs(001) surface freshly passivated by the TAM treatment: ≈1.5 ML of In-S, ≈1.2 ML of In-O_x, 0.2–0.4 ML of As-O_x, and possibly up to 0.2 ML of As-S. After 42 days in air, both As-O_x and S coverages were slightly above 1 ML. In addition to offering superior properties potentially useful in practical surface passivation, the TAM passivation clearly produces excellent model S-passivated InAs(001) surfaces. The quantitative XPS data and analysis, as well as the DL model and empirical coverage calibration developed and validated on these model surfaces will be useful as a benchmark and quantitative reference in studies of passivated InAs interfaces with more complex structures.

Acknowledgements

D. Y. P. thanks Dr Jennifer C. Sullivan (NRL) for providing the XPS data of the native-oxide InAs(001) control and for helpful discussions of surface chemistry and quantitative XPS analysis of functionalized III-V semiconductors. The work was supported by the Office of Naval Research, the Air Force Office of Scientific Research, and the Defense Advanced Research Projects Agency.

APPENDIX: EAL CALCULATIONS

The EAL values used for quantitative XPS analysis were calculated using the NIST SRD-82 software.[21,22] The software relies on the TPP-2M formula[24] for calculating inelastic mean free path (IMFP) values. A previous study has shown that the TPP-2M predictions for InAs were in good agreement with IMFPs experimentally measured in InAs,[25] which can be considered a good independent reliability test of the TPP-2M-based EAL calculations for this material. The uncertainty of the calculated EAL values is estimated by the authors of the software to be ≈20%.[22] The validity of the TPP-2M predictive formula and SRD-82 EAL calculations has been established for photoelectrons with KE > 200 eV,[22,24] and has been recently extended down to KE > 50 eV for elemental solids,[26] but for the As $2p_{3/2}$ photoelectrons (KE ≈ 160 eV) in InAs there could be some effects unaccounted for in the model.

The material parameters required by the software for the EAL calculations include the chemical composition (stoichiometry), density ρ, photoionization asymmetry parameter β, and band gap energy E_g. For the InAs substrate, we assumed the bulk InAs 1:1 stoichiometry, and the standard values for $\rho = 5.68\ \mathrm{g/cm^3}$ and $E_g = 0.4$ eV. For the overlayers, the uncertainty about their actual structure and composition required some simplifying assumptions. For overlayer density, the bulk InAs value is close to the average of values reported for different In and As oxides (about 7 and 4 $\mathrm{g/cm^3}$, respectively); therefore, we assumed the density to be the same for the substrate and overlayer. Reported E_g values for In and As oxides are primarily within the 3–4 eV range;[27] therefore, we assumed $E_g = 3.5$ eV for the overlayer. The EALs calculated for the +5 oxide stoichiometry differed from those for the +3 oxide by <5%; therefore, for simplicity, we assumed the +3 oxide stoichiometry (In : As : O = 1 : 1 : 3) for the overlayer. In another simplification, the EALs calculated for the oxide were also used to quantify the S overlayer. In all cases, the EALs calculated for the overlayer differed from those for the InAs substrate by <15%; thus, we expect that the simplified treatment of the overlayer material parameters did not significantly affect the overall uncertainty while capturing the principal effect of the overlayer chemistry on the attenuation of photoelectrons.

We used the SRD-82 software to calculate two EAL values for each elemental peak (Table A1): ''EAL for quantitative analysis'' (QEAL) and ''average practical EAL'' (PEAL). The formal definitions of these two parameters are given in Ref. 21, but the practical implications can be summarized as follows: QEAL is essentially a property of a semi-infinite slab of material and thus is used in all pre-exponential factors, whereas the PEAL relates to attenuation by the overlayer and thus is used in the exponential attenuation terms. We actually use the 'average' PEAL, i.e. PEAL averaged over a certain overlayer thickness (0.4 nm). The average PEALs calculated for a 1.5 nm overlayer thickness differed from these by <5%. As a reference, the bulk InAs lattice constant is 0.606 nm.

Two factors can potentially affect XPS data measured using single-crystal InAs substrates: photoelectron diffraction and coherent inelastic scattering. These single-crystal effects primarily occur for high-KE photoelectrons that propagate through multiple ordered atomic layers before being emitted. Conversely, for the low-KE As 2p photoelectrons that originate in a top few relatively disordered atomic layers, any single-crystal effects will be minimal. Similarly, all photoelectrons originating in the near-surface layers will not be affected: for InAs-S this includes the S 2p peak, and the As-O_x, In-O_x, In-S surface components. Thus, the only peaks considered in our study that could be affected by the use of single-crystal substrates are the 'bulk' As-In and In-As 3d peaks. The Scofield-adjusted[23] As/In ratios calculated from these 'bulk' components were 0.97 ± 0.06 (normal emission) and 1.00 ± 0.07 (65° emission) for samples in our study. The

Table A1. Calculated values of PEAL in the oxide overlayer and QEAL in bulk InAs

Peak	KE (eV)	Asymmetry parameter β	Emission angle (°)	PEAL L_{ox} (nm)	QEAL L_b^Q (nm)
As 3d	1445	1.055	0	2.26	3.11
			35	2.26	3.09
			65	2.27	3.02
In $3d_{5/2}$	1042	1.22	0	1.72	2.43
			35	1.72	2.41
			65	1.73	2.35
As $2p_{3/2}$	162	1.131	0	0.458	0.691
			35	0.458	0.685
			65	0.476	0.664
As $2p_{1/2}$	127	1.131	0	0.407	0.615
			35	0.406	0.609
			65	0.426	0.531

variation in these ratios is comparable to the uncertainty of fitting the In-As components; therefore, the variability in the azimuths of detected photoelectrons caused by sample positioning did not significantly affect the results of angle-integrated or angle-resolved measurements. This result is consistent with previous systematic studies that have demonstrated a rather small variation of As 3d/Ga 3d ratios caused by orientation effects in single-crystal GaAs(001) (~10% near normal emission, ~20% around 65° emission).[28,29] The As 3d photoelectrons have KE higher than the In 3d (or Ga 3d) photoelectrons, so a simple model of emission from a semi-infinite stack of alternating In and As atomic planes predicts an experimental As/In ratio larger than unity. Our experimental As/In ratio is smaller than this prediction, indicating that the As 3d intensity may be suppressed, likely because of the single-crystal effects (potentially both diffraction and inelastic scattering).[30] Accordingly, we do not use the As 3d intensity in quantification of the absolute AsO_x and S coverages.

REFERENCES

1. Sandroff CJ, Nottenburg RN, Bischoff JC, Bhat R. *Appl. Phys. Lett.* 1987; **51**: 33.
2. Fan JF, Oigawa H, Nannichi Y. *Jpn. J. Appl. Phys.* 1988; **27**: L1331.
3. Oigawa H, Fan JF, Nannichi Y, Sugahara H, Oshima M. *Jpn. J. Appl. Phys.* 1991; **30**: L322.
4. Bessolov VN, Lebedev MV. *Semiconductors* 1998; **32**: 1141.
5. Lebedev MV. *Prog. Surf. Sci.* 2002; **70**: 153.
6. Seker F, Meeker K, Kuech TF, Ellis AB. *Chem. Rev.* 2000; **100**: 2505.
7. Petrovykh DY, Yang MJ, Whitman LJ. *Surf. Sci.* 2003; **523**: 231.
8. Lu ED, Zhang FP, Xu SH, Yu XJ, Xu PS, Han ZF, Xu FQ, Zhang XY. *Appl. Phys. Lett.* 1996; **69**: 2282.
9. Xu FQ, Lu ED, Pan HB, Xie CK, Xu PS, Zhang XY. *Surf. Rev. & Lett.* 2001; **8**: 19.
10. Canali L, Wildoer JWG, Kerkhof O, Kouwenhoven LP. *Appl. Phys. A* 1998; **66**: S113.
11. Petrovykh DY, Long JP, Whitman LJ. *Appl. Phys. Lett.* 2005; **86**: 242105.
12. Petrovykh DY, Kimura-Suda H, Tarlov MJ, Whitman LJ. *Langmuir* 2004; **20**: 429.
13. Hesse R, Chasse T, Szargan R. *Fresenius J. Anal. Chem.* 1999; **365**: 48.
14. Poirier DM, Weaver JH. *Surf. Sci. Spectra* 1993; **2**: 224.
15. Fukuda Y, Suzuki Y, Sanada N, Shimomura M, Masuda S. *Phys. Rev. B* 1997; **56**: 1084.
16. Ichikawa S, Sanada N, Utsumi N, Fukuda Y. *J. Appl. Phys.* 1998; **84**: 3658.
17. Katayama M, Aono M, Oigawa H, Nannichi Y, Sugahara H, Oshima M. *Jpn. J. Appl. Phys.* 1991; **30**: L786.
18. Mihailova T, Velchev N, Krastev V, Marinova T. *Appl. Surf. Sci.* 1997; **120**: 213.
19. Hollinger G, Skheytakabbani R, Gendry M. *Phys. Rev. B* 1994; **49**: 11159.
20. Lebedev MV, Mayer T, Jaegermann W. *Semiconductors* 2004; **38**: 153.
21. Jablonski A, Powell CJ. *Surf. Sci. Rep.* 2002; **47**: 35.
22. Powell CJ, Jablonski A. *NIST Electron Effective-Attenuation-Length Database, Version 1.0 (SRD-82)*, US Department of Commerce, National Institute of Standards and Technology: Gaithersburg, MD, 2001.
23. Scofield JH. *J. Electron Spectrosc. Relat. Phenom.* 1976; **8**: 129.
24. Tanuma S, Powell CJ, Penn DR. *Surf. Interface Anal.* 1994; **21**: 165.
25. Gergely G, Menyhard M, Gurban S, Benedek Z, Daroczi C, Rakovics V, Toth J, Varga D, Krawczyk M, Jablonski A. *Surf. Interface Anal.* 2000; **30**: 195.
26. Tanuma S, Powell CJ, Penn DR. *Surf. Interface Anal.* 2005; **37**: 1.
27. Kuryshev GL, Kovchavtsev AP, Valisheva NA. *Semiconductors* 2001; **35**: 1063.
28. Alnot P, Olivier J, Wyczisk F, Fadley CS. *J. Electron Spectrosc. Relat. Phenom.* 1987; **43**: 263.
29. Alnot P, Olivier J, Fadley CS. *J. Electron Spectrosc. Relat. Phenom.* 1989; **49**: 159.
30. Seah MP, Spencer SJ. *Surf. Interface Anal.* 2002; **33**: 640.